Direct and indirect characterization of electrocaloric effect in (Na,K)NbO_3 based lead-free ceramics

Jianting Li,[1] Yang Bai,[1,a)] Shiqiang Qin,[1] Jian Fu,[2] Ruzhong Zuo,[2,b)] and Lijie Qiao[1]
[1]*Key Laboratory of Environmental Fracture, Ministry of Education, University of Science and Technology Beijing, Beijing 100083, China*
[2]*Institute of Electro Ceramics and Devices, School of Materials Science and Engineering, Hefei University of Technology, Hefei 230009, China*

(Received 6 September 2016; accepted 7 October 2016; published online 18 October 2016)

This paper demonstrated the electrocaloric effect (ECE) of $(Na_{0.52}K_{0.48-x})(Nb_{0.92-x}Sb_{0.08})O_3$-$xLiTaO_3$ lead-free ceramics by direct differential scanning calorimetry measurement and indirect thermodynamic method. Both results show good consistency, where the direct one more accurately depicts ECE value and its evolution according to phase diagram. Due to the diffuse orthorhombic-tetragonal phase transition, the samples show a broad ECE peak which shifts to lower temperature with increasing $LiTaO_3$ amount. Compared to previous direct results in lead-free ceramics at corresponding temperatures, they show a competitive ECE performance with ΔT_{max} of 0.41 K (@80 °C), 0.30 K (@35 °C) and 0.16 K (@15 °C) under 20 kV/cm fields for x = 0.02, 0.0375 and 0.045. *Published by AIP Publishing.* [http://dx.doi.org/10.1063/1.4965707]

Ferroelectric ceramics are one of the most important functional materials for microelectronic technology, owing to their excellent dielectric, ferroelectric, and piezoelectric performances.[1] Recently, ferroelectric refrigeration based on electrocaloric effect (ECE) becomes a hot topic in ferroelectric scope.[2] Due to special advantages of high efficiency, easy miniaturization, and feasible manipulation,[3,4] it offers the best refrigeration solution for microelectronic and microelectromechanical systems, in which local high temperature has become the primary factor of failure.

ECE refers to a reversible adiabatic temperature change and/or isothermal entropy change when an electric field is applied on or removed from a polar material. Although lead based ferroelectric ceramics exhibit excellent polarization features, Pb toxicity and volatility make their applications restricted, so that lead-free ferroelectric ceramics attracted more attentions for increasingly stringent environmental requirement.[5–12] (Na,K)NbO_3 (NKN) based ceramics are a distinguished family of lead-free ferroelectrics and a lot of works have been done to optimize piezoelectric and ferroelectric properties,[13–15] but their ECE has been never explored so far. This paper was focused on the ECE of Li, Ta, and Sb modified NKN lead-free ceramics, $(Na_{0.52}K_{0.48-x})(Nb_{0.92-x}Sb_{0.08})O_3$-$xLiTaO_3$ (NKNS-xLT, $0.01 < x < 0.045$), which exhibited excellent ferroelectric and piezoelectric properties in previous work[14,15] and were also expected to be a good ECE candidate material. For ECE characterization, the indirect thermodynamic method is the most widely used due to simple testing setup and operation but it fails in many cases such as for nonergodic relaxor or under ultrahigh fields;[4,16–19] while the direct heat flow measurement using differential scanning calorimeter (DSC) has the best accuracy for bulk samples at the expense of time efficiency.[20–26] In this work, direct DSC measurement and indirect thermodynamic method were both adopted to characterize the ECE property of NKNS-xLT ceramics solidly.

NKNS-xLT ($0.01 < x < 0.045$) ceramics were prepared by a conventional solid state process, as described in Ref. 14. X-ray diffraction (XRD) results confirmed that all samples have a pure perovskite structure. Dielectric measurement was carried out at different temperatures using an LCR meter (Agilent E4980A). The ferroelectric hysteresis loops were measured at 10 Hz within 20–120 °C using a ferroelectric analyzer (aixACCT TF2000). Based on the thermodynamic Maxwell relation, the ECE adiabatic ΔT was calculated using the following formula:

$$\Delta T = -\frac{T}{\rho C}\int_{E_1}^{E_2}\left(\frac{\partial P}{\partial T}\right)dE, \tag{1}$$

where $\boldsymbol{\rho}$ is the measured density by Archimedes method, $\boldsymbol{C}$ is the heat capacity under constant electric fields. The direct ECE measurement was performed in an isothermal process (−20–100 °C) using a modified DSC (TA Instruments Q2000), and a DC power supplier (Trek 677B) was used to apply electric fields on the sample.

Fig. 1 shows the temperature dependence of dielectric permittivity for the samples with x = 0.02, 0.0375 and 0.04. All samples show a distinct dielectric peak around 250 °C, which refers to the transition from tetragonal ferroelectric phase to cubic paraelectric phase. There is another dispersive peak below 100 °C, corresponding to the orthorhombic-tetragonal (O-T) phase transition, as evidenced by XRD results.[15] It gradually shifts to lower temperature with increasing LT amount, 80 °C for NKNS-0.02LT, 30 °C for NKNS-0.0375LT, and 15 °C for NKNS-0.04LT. Due to the remarkable diffuse character, the O-T phase transition does not produce endothermic peak and latent heat in the DSC heat flow curves, as shown in Fig. 2. Because the O-T transition is closer to room temperature, it will be more desired in

a)Author to whom correspondence should be addressed. Electronic mail: baiy@mater.ustb.edu.cn. Fax: 86-10-62332345.
b)Electronic mail: piezolab@hfut.edu.cn. Fax: 86-551-2905285.

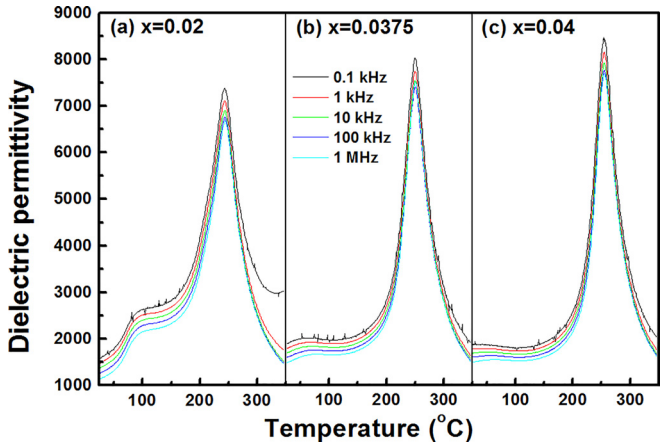

FIG. 1. Temperature dependence of dielectric permittivity for NKNS-xLT ceramics. (a) x = 0.02; (b) x = 0.0375; (c) x = 0.045.

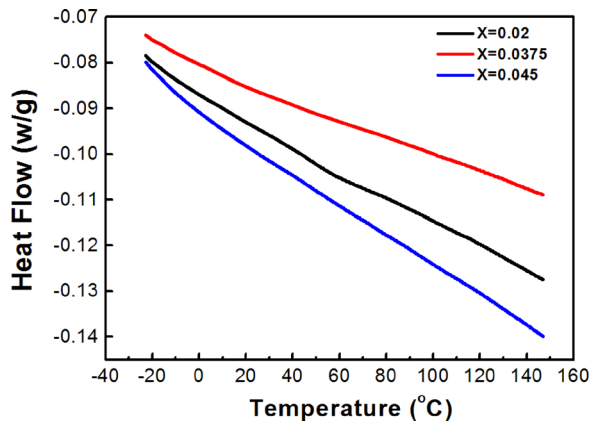

FIG. 2. DSC heat flow curves of NKNS-xLT ceramics.

applications. And our previous work proved O-T transition can also provide large ECE.[22] Then the following discussions were more focused on the O-T transition.

Fig. 3 shows the P-E loops of NKNS-xLT ceramics measured at different temperatures. All samples show typical ferroelectric hysteresis loops and have polarization approaching 30 μC/cm^2 at room temperature, much larger than that of $BaTiO_3$ based ceramics.[12,23–30] With the rise of temperature, the polarization monotonically drops. On one hand, the thermal agitation increasingly destroys the order arrangement of dipoles; on the other hand, dipole moment changes with the O-T transition.

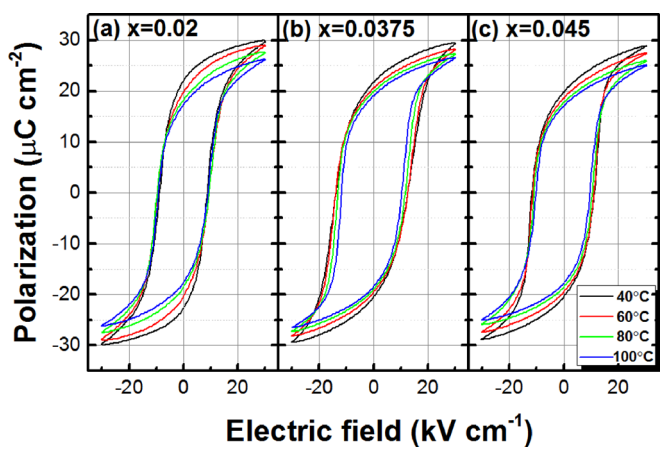

FIG. 3. Ferroelectric hysteresis loops under different temperatures for NKNS-xLT ceramics.

The ECE properties of NKNS-xLT ceramics were characterized by both direct ECE measurement and indirect thermodynamic method. Fig. 4 shows a typical heat flow curve directly measured under different electric fields in an isotropic process (NKNS-0.0375LT, at 10 °C), where exothermic peaks refer to the application of electric fields and endothermic peaks to the removal of fields. The exothermic or endothermic peaks are of uniform magnitude in continuous repeated cycles, which were elevated under higher fields (Fig. 5). It is also noted that the exothermic values are slightly higher than the endothermic value, especially under higher fields, which is attributed to energy dissipation in dipolar switching and Joule heat.[31,32] Here, the cause of Joule heat is not leakage current but polarization current, where the former is a continuous effect and the latter a transient effect. Since the sintered ceramic samples have very high resistivity ($>10^{12}$ Ω cm), the leakage current can be neglected, which is also confirmed by the fact that the heat flow well returns to the horizontal baseline after each change of electric fields. This is a reason for the larger exothermic peak in the initial cycle. The ECE isotropic ΔS is directly obtained by the integral area of exothermic or endothermic peaks, further the adiabatic ΔT.

The direct and indirect ECE results are shown Fig. 6. The indirect thermodynamic results were calculated based on the P-T curves, as shown in Figs. 6(a), 6(c) and 6(e). For NKNS-0.02LT, there is a wide ECE peak with $\Delta T_{max} = 0.55$ K (30 kV/cm) at 68 °C. The direct result (Fig. 6(b)) agrees with the indirect one well, except that the peak (0.41 K@20 kV/cm) shifts to higher temperature of 80 °C. Previous references proved that the ECE peak originates from the ferroelectric phase transition and occurs close to the transition temperature. Compared with the dielectric results showing a dielectric anomaly at ~80 °C, the direct measurement presents more convincing results for theoretical analysis. For NKNS-0.0375LT, the indirectly obtained ECE peak occurs at 40 °C and has a maximum of $\Delta T_{max} = 0.41$ K under 30 kV/cm. The direct result (Fig. 6(d)) shows a high consistency with the indirect one, except for a slight shift also. For NKNS-0.045LT, the linear and monotonic variation of polarization implies a steady ECE, that is. flat ΔT-T curves, meaning that the ECE peak is out of the experiment temperature range. The

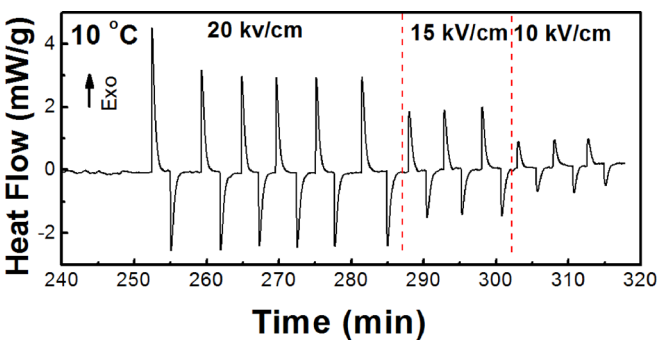

FIG. 4. Typical DSC heat flow curve of direct ECE measurements under different electric fields in an isotropic process, where the selected specimen is NKNS-0.0375LT and T = 10 °C.

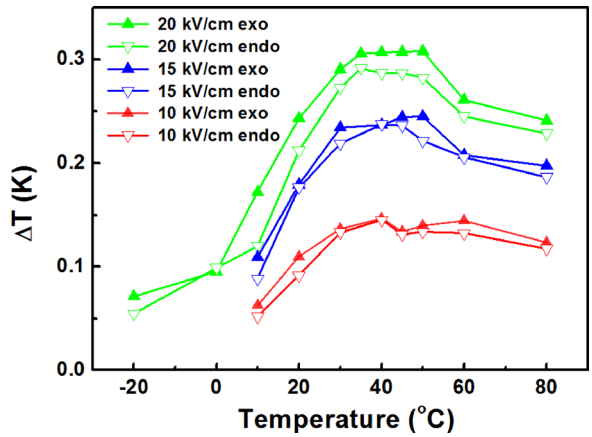

FIG. 5. Temperature dependence of direct measured ECE ΔT under different electric fields for NKNS-0.0375LT.

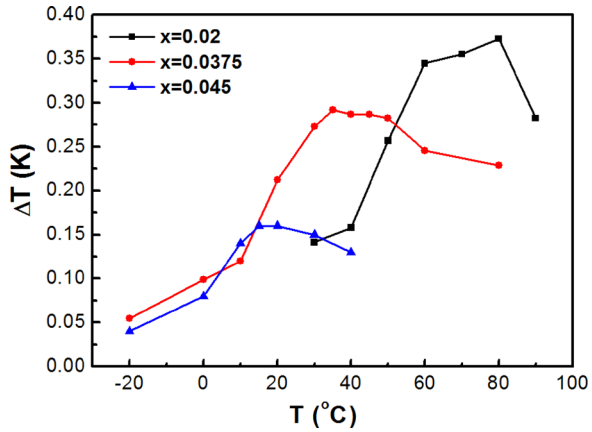

FIG. 7. Comparison of ECE ΔT direct measured under 20 kV/cm electric fields for NKNS-xLT ceramics.

fluctuation in the ΔT-T curves originates from the process of polynomial fitting, which often produces artifacts in some indirect calculations. The direct result (Fig. 6(f)) depicts the whole ΔT-T curves with a peak at 15 °C, which coincides with the dielectric results.

Direct ECE data for all samples are gathered in Fig. 7. With the rise of LT amount, the ECE peak gradually reduces and shifts to lower temperature, which agrees with the phase diagram.[14] The x = 0.02, 0.0375 and 0.045 samples show ECE ΔT_{max} of 0.41 K (@80 °C), 0.30 K (@35 °C) and 0.16 K (@15 °C) under 20 kV/cm fields, respectively.

Within the temperature range from RT to 100 °C, most desired by applications, NKNS-xLT has a competitive ECE performance compared with previous directly measured results in lead-free ferroelectric ceramics. The magnitude of ECE ΔT is comparable to or higher than those in $BaTiO_3$ or $(Na_{0.5}Bi_{0.5})TiO_3$ based ceramics, such as $Ba_{0.7}Sr_{0.3}TiO_3$ ($\Delta T_{max} = 0.18$ K @10 kV/cm and @15 °C),[23] $0.65Ba(Zr_{0.2}Ti_{0.8})O_3$-$0.35(Ba_{0.7}Ca_{0.3})TiO_3$ ($\Delta T_{max} = 0.33$ K @20 kV/cm and @65 °C)[24] and $0.82(Na_{0.5}Bi_{0.5})TiO_3$-$0.18(K_{0.5}Bi_{0.5})TiO_3$ (ΔT = 0.25 K @22 kV/cm and @100 °C).[25] It is also noted that the ECE peak is very broad due to remarkable diffuse feature, which facilities the applications.

In summary, we studied the ECE property of the NKNS-XLT (x = 0.02, 0.0375, 0.045) lead-free ceramics by direct and indirect methods. The ECE property directly obtained by DSC heat flow measurement agrees with that calculated by indirect thermodynamic method very well. The direct measurement provides more accurate ECE data and depicts a clearer ECE evolution with temperature and composition following phase diagram. All samples show a broad ECE peak due to a diffuse orthorhombic-tetragonal phase transition, whose position shifts to lower temperature with increasing LT amount. The samples exhibit a competitive ECE performance within a wide temperature scope from RT to 100 °C. Moreover, it should be noted that the O-T phase transition is involved in this work. If the ferroelectric-paraelectric phase transition is adopted, much higher ECE performance may be

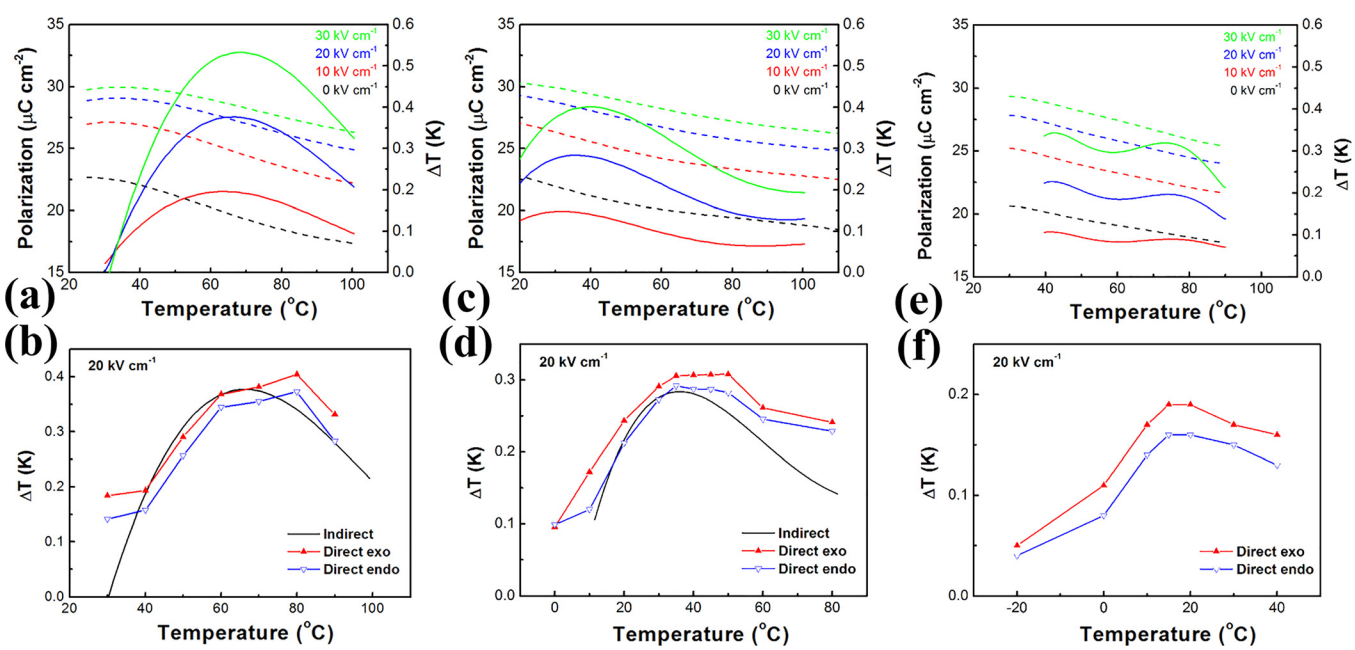

FIG. 6. ECE property of NKNS-xLT ceramics by indirect method (a), (c), (e) and direct measurement (b), (d), (f). (a), (b) x = 0.02, (c), (d) x = 0.0375, (e), (f) x = 0.045. Temperature dependences of polarization measured under different electric fields are also shown in (a), (c), (e).

achieved due to larger configurational entropy. Hence, NKN based lead-free ceramics provide a promising candidate for environmental friendly solid-state cooling technology.

This work was supported by grants from the National Science Foundation of China (51372018).

[1]J. F. Scott, Science **315**, 954–959 (2007).
[2]M. Valant, Prog. Mater. Sci. **57**, 980–1009 (2012).
[3]S. G. Lu and Q. M. Zhang, Adv. Mater. **21**, 1983–1987 (2009).
[4]Y. Bai, G. P. Zheng, and S. Q. Shi, Appl. Phys. Lett. **96**, 192902 (2010).
[5]Y. Saito, H. Takao, T. Tani, T. Nonoyama, K. Takatori, T. Homma, T. Nagaya, and M. Nakamura, Nature **432**, 84–87 (2004).
[6]R. Z. Zuo, X. S. Fang, and C. Ye, Appl. Phys. Lett. **90**, 092904 (2007).
[7]W. Liu and X. Ren, Phys. Rev. Lett. **103**, 257602 (2009).
[8]J. G. Wu, D. Q. Xiao, and J. G. Zhu, Chem. Rev. **115**, 2559–2595 (2015).
[9]F. Z. Yao, K. Wang, W. Jo, K. G. Webber, T. P. Comyn, J. X. Ding, B. Xu, L. Q. Cheng, M. P. Zheng, Y. D. Hou, and J. F. Li, Adv. Funct. Mater. **26**, 1217–1224 (2016).
[10]H. Chen, T. Ren, X. Wu, Y. Yang, and L. Liu, Appl. Phys. Lett. **94**, 182902 (2009).
[11]Y. Bai, G. P. Zheng, and S. Q. Shi, Mater. Res. Bull. **46**, 1866–1869 (2011).
[12]Y. Bai, X. Han, and L. J. Qiao, Appl. Phys. Lett. **102**, 252904 (2013).
[13]R. Z. Zuo and J. Fu, J. Am. Ceram. Soc. **94**, 1467–1470 (2011).
[14]R. Z. Zuo, J. Fu, and D. Lv, J. Am. Ceram. Soc. **92**, 283–285 (2009).
[15]J. Fu and R. Z. Zuo, Appl. Phys. Lett. **102**, 122902 (2013).
[16]D. Guyomar, G. Sebald, B. Guiffard, and L. Seveyrat, J. Phys. D: Appl. Phys. **39**, 4491–4496 (2006).
[17]S. G. Lu, B. Rozic, Q. M. Zhang, Z. Kutnjak, X. Y. Li, E. Furman, L. J. Gorny, M. R. Lin, B. Malic, M. Kosec, R. Blinc, and R. Pirc, Appl. Phys. Lett. **97**, 162904 (2010).
[18]R. Chukka, J. W. Cheah, Z. Chen, P. Yang, S. Shannigrahi, J. Wang, and L. Chen, Appl. Phys. Lett. **98**, 242902 (2011).
[19]R. Pirc, Z. Kutnjak, R. Blinc, and Q. M. Zhang, J. Appl. Phys. **110**, 074113 (2011).
[20]G. Sebald, S. Pruvost, L. Seveyrat, L. Lebrun, D. Guyomar, and B. Guiffard, J. Eur. Ceram. Soc. **27**, 4021–4024 (2007).
[21]Y. Bai, G. P. Zheng, K. Ding, L. J. Qiao, S. Q. Shi, and D. Guo, J. Appl. Phys. **110**, 094103 (2011).
[22]Y. Bai, K. Ding, G. P. Zheng, S. Q. Shi, J. L. Cao, and L. J. Qiao, AIP Adv. **2**, 022162 (2012).
[23]Y. Bai, X. Han, K. Ding, and L. J. Qiao, Appl. Phys. Lett. **103**, 162902 (2013).
[24]M. Sanlialp, V. V. Shvartsman, M. Acosta, B. Dkhil, and D. C. Lupascu, Appl. Phys. Lett. **106**, 062901 (2015).
[25]F. Le Goupil, J. Bennett, A. K. Axelsson, M. Valant, A. Berenov, A. J. Bell, T. P. Comyn, and N. McN. Alford, Appl. Phys. Lett. **107**, 172903 (2015).
[26]J. N. Li, D. W. Zhang, S. Q. Qin, T. Y. Li, M. Wu, D. Wang, Y. Bai, and X. J. Lou, Acta Mater. **115**, 58–67 (2016).
[27]Z. D. Luo, D. W. Zhang, Y. Liu, D. Zhou, Y. G. Yao, C. Q. Liu, B. Dkhil, X. B. Ren, and X. J. Lou, Appl. Phys. Lett. **105**, 102904 (2014).
[28]F. Han, Y. Bai, L. J. Qiao, and D. Guo, J. Mater. Chem. C **4**, 1842–1849 (2016).
[29]Y. H. Sun, Z. Li, H. F. Zhang, C. Y. Yu, G. Viola, S. Fu, V. Koval, and H. X. Yan, Mater. Lett. **175**, 79–81 (2016).
[30]H. Kaddoussi, A. Lahmar, Y. Gagou, B. Asbani, J. L. Dellis, G. Cordoyiannis, B. Allouche, H. Khemakhem, Z. Kutnjak, and M. El Marssi, J. Alloys Compd. **667**, 198–203 (2016).
[31]M. Valant, A. K. Axelsson, F. Le Goupil, and N. McN. Alford, Mater. Chem. Phys. **136**, 277–280 (2012).
[32]C. Molin, M. Sanlialp, V. V. Shvartsman, D. C. Lupascu, P. Neumeister, A. Schönecker, and S. Gebhardta, J. Eur. Ceram. Soc. **35**, 2065–2071 (2015).